# Synchrotron X-ray Diffraction Study of Microtubules Buckling and Bundling under Osmotic Stress: A Probe of Interprotofilament Interactions

Daniel J. Needleman,[1,2] Miguel A. Ojeda-Lopez,[1,2] Uri Raviv,[1,2] Kai Ewert,[1,2] Jayna B. Jones,[1,2] Herbert P. Miller,[2] Leslie Wilson,[2] and Cyrus R. Safinya[1,2,*]

[1]*Materials Department, Physics Department, University of California, Santa Barbara, California 93106, USA*
[2]*Molecular, Cellular, & Development Biology Department, University of California, Santa Barbara, California 93106, USA*
(Received 21 April 2004; published 4 November 2004)

Microtubules are hollow cylinders composed of tubulin heterodimers that stack into linear protofilaments that interact laterally to form the microtubule wall. Synchrotron x-ray diffraction of microtubules under increasing osmotic stress shows they transition to rectangular bundles with noncircular buckled cross sections, followed by hexagonally packed bundles. This new technique probes the strength of interprotofilamen bonds, yielding insight into the mechanism by which associated proteins and the chemotherapy drug taxol stabilize microtubules.

DOI: 10.1103/PhysRevLett.93.198104 PACS numbers: 87.16.Ka, 61.10.Eq, 61.30.Eb, 61.30.St

Microtubules (MTs), a major component of the eukaryotic cytoskeleton, are protein polymers involved in a range of functions including mitosis, cell motility, and intracellular transport. $\alpha\beta$ tubulin heterodimers align end to end into protofilaments that form the MT wall (Fig. 1). Protofilaments form sheets at the ends of growing MTs, but curl and peel apart from each other at the ends of shortening MTs, eventually detaching as highly curved oligomers [1]. Thus, the curvature of protofilaments and the interactions between them are thought to be crucial for MT polymerization and depolymerization. The forces that stabilize tubulin in the MT lattice and control MT dynamics are not well understood.

MT dynamics are regulated by microtubule associated proteins (MAPs) *in vivo*, causing some MTs to rapidly shorten and grow, such as those in the mitotic spindle, while others form stable structures, like those in the axons of nerve cells [1]. In a number of neurodegenerative diseases, incorrectly phosphorylated MAPs lead to altered MAP-MT interactions with detrimental consequences for cellular activity [2]. It is unclear if MT stabilizing MAPs function by cross-linking tubulin dimers, laterally, longitudinally, or in a more complex fashion, or by causing a conformational change in tubulin [1]. Similarly, a variety of anticancer drugs currently in use in clinical chemotherapy procedures function by interfering with MT dynamics, yet the mechanisms by which these agents affect MT stability are poorly understood. For example, the microscopic mode of action of the drug taxol, which prevents cell division by binding to and stabilizing MTs, is unknown [3]. It has been proposed that taxol may stabilize MTs by either increasing the lateral interactions between protofilaments or locking the tubulin dimers in a straight conformation [4].

We report on a synchrotron small angle x-ray diffraction (SAXRD) study of MTs subjected to osmotic stress [5] and depletion attraction [6] due to added poly-(ethylene-oxide) (PEO) and show that solutions of MTs undergo two transitions. First, above a critical osmotic pressure, $P_{cr}$, MTs are found to exhibit a buckling transition, distorting and forming bundles with rectangular lattice symmetry. The $P_{cr}$ of $\sim$600 Pa provides the first measurement of the strength of lateral bonds between protofilaments within a MT. The MTs distort further with increasing osmotic pressure. The buckling transition and the continued deformation of MTs, both of which are fully reversible, give detailed information on the mechanical properties of MTs. Second, for higher concentrations of PEO the polymer enters the MT lumen, resulting in a transition to a hexagonal array of unbuckled MTs. In this hexagonal phase, we have used the SAXRD-osmotic stress technique [5] to measure interactions between MTs, thus paving the way for studies that will determine how MAPS alter MT-MT interaction. Our study provides the first direct evidence that some MAPs increase lateral interactions between protofilaments

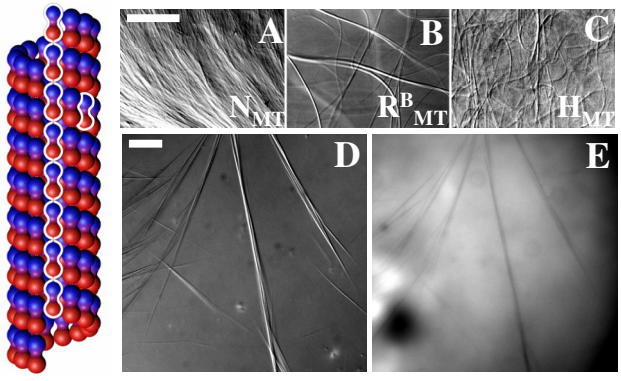


FIG. 1 (color online). A MT with a tubulin heterodimer and protofilament outlined. DIC of (a) a nematic of MTs with no PEO, (b) rectangular bundles of MTs with 1% (w/w) 20k PEO, and (c) MTs in hexagonal bundles with 20% 20k PEO. DIC (d) and the corresponding fluorescence (e) of the rectangular phase with fluorescently labeled 20k PEO 10$\mu$m scale bars.

  

whereas taxol does not. Methods introduced in this Letter should enable the elucidation of drug-MT and MAP-MT interactions.

MTs were polymerized from 40 $\mu$M tubulin with 1 mM guanine triphosphate (GTP) and subsequentially stabilized with taxol. Solutions with MTs were mixed with an equal volume of solutions of PEO, an inert polymer that shows an unfavorable thermodynamic interaction with tubulin [7]. MTs do not bundle with low amounts of PEO of molecular weight 20 000 g/mol (20k PEO) , but orient at high MT concentrations [differential interference contrast (DIC) optical micrograph, Fig. 1(a)]. We refer to this oriented state as a nematic with long-range orientational order, even though the phase may not have reached equilibrium. At intermediate concentrations of 20k PEO, thick, highly refractive bundles of MTs appear [Fig. 1(b)], while for large amounts of added 20k PEO smaller bundles are visible [Fig. 1(c)]. Synchrotron SAXRD reveals dramatically different structural organization of the MTs corresponding to the low, intermediate, and high 20k PEO concentration regimes. At 0.2% (w/w) 20k PEO (Fig. 2, bottom curve, labeled $N_{\mathrm{MT}}$) the SAXRD of samples corresponding to the image of Fig. 1(a) is consistent with the form factor of single MTs with $\sim$13 protofilaments [8], which is expected for MTs stabilized by taxol after polymerization [4], as these were.

At intermediate concentrations (1% 20k PEO), corresponding to the DIC image of Fig. 1(b), SAXRD reveals a highly ordered bundled phase of MTs (Fig. 2, labeled $R^{\mathrm{B}}_{\mathrm{MT}}$). Surprisingly, the observed nine orders of diffraction peaks seen with 1% 20k PEO are found to index exactly on a 2D *rectangular lattice* where one of the lattice spacings is *smaller* than the unperturbed MT diameter of 25.4 nm (Fig. 2, curves labeled $R^{\mathrm{B}}_{\mathrm{MT}}$ with lattice parameters $a_R = 2\pi/q_{01} = 18.47$ nm and $b_R = 2\pi/q_{10} = 33.40$ nm). This rectangular $R^{\mathrm{B}}_{\mathrm{MT}}$ phase consists of MTs whose cross sections have buckled from a circular to a noncircular shape. We surmise that these MTs are elliptical in cross section as predicted in simulations and by analytical theory for small deformations, and not biconcave [9]. The latter is expected at higher pressures [9], but would result in a *distorted* rectangular lattice. The buckling is reversible: if MTs in the rectangular phase are sedimented by centrifugation and resuspended in a buffer without PEO, these same MTs become unbundled and form a nematic phase of unbuckled, undamaged MTs as determined by SAXRD. This reversibility shows that MTs in the rectangular phase are intact with no change in protofilament number.

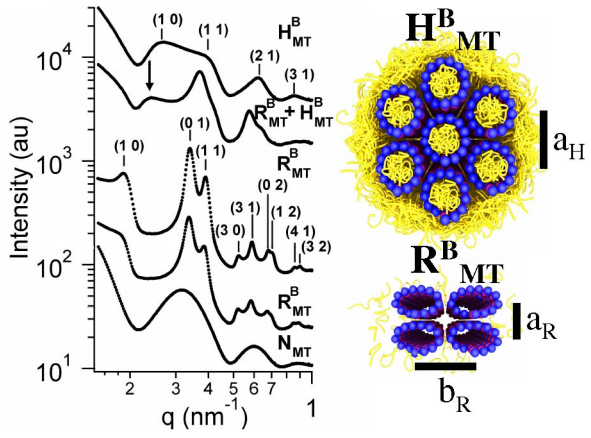


FIG. 2 (color online). SAXRD of MTs with 20k PEO. MTs in the nematic phase with 0.2% (w/w) 20k PEO ($N_{\mathrm{MT}}$). With 1% 20k PEO ( $R^{\mathrm{B}}_{\mathrm{MT}}$, lower plot), SAXRD shows a rectangular lattice. With 25 mM KCl and 1% 20k PEO ( $R^{\mathrm{B}}_{\mathrm{MT}}$, upper plot) the peaks become sharper and the (1 0) peak is clearly visible. With 7.5% 20k PEO ($R^{\mathrm{B}}_{\mathrm{MT}} + H_{\mathrm{MT}}$), there is coexistence between the hexagonal [(1 0) peak indicated by arrow] and rectangular bundles. With 20% 20k PEO ($H_{\mathrm{MT}}$), only the hexagonal phase is present. Cartoons display MT cross sections from the bundle phases.

At high PEO concentrations (20% 20k PEO) as in Fig. 1(c), SAXRD displays four Bragg peaks showing 2D hexagonal symmetry, implying a bundled phase of hexagonally packed undistorted MTs (Fig. 2, top curve, labeled $H^{\mathrm{B}}_{\mathrm{MT}}$ with lattice parameter $a_H = 4\pi/\sqrt{3}q_{10} = 26.97$ nm). Thus, the MT shape exhibits a reentrant behavior from circular to noncircular and back to circular as a function of increasing PEO. At slightly lower concentrations (7.5% 20k PEO), SAXRD shows a coexistence of rectangular and hexagonal bundles (Fig. 2, labeled $R^{\mathrm{B}}_{\mathrm{MT}} + H^{\mathrm{B}}_{\mathrm{MT}}$). Both bundle phases are formed by depletion attraction induced by the PEO [6].

The surprising transition from buckled to unbuckled MTs with *increasing* 20k PEO concentration can be understood by noting that the radius of gyration of 20k PEO, $\sim$7 nm [10], is only slightly smaller than the inner radius of the MT, $\sim$8.7 nm [11]. For low amounts of 20k PEO, it is expected that the polymer will not enter the MT lumen, due to the entropic cost of confining the PEO. If PEO is modeled as a Gaussian chain and the MTs as hollow cylinders, then the concentration of polymer in the MTs should be less than 2% of the bulk concentration [12], and the pressure difference between the inside and the outside causes the MTs to buckle. At higher concentrations of polymer, near the overlap concentration $c = c^* \sim 7.5\%$ (w/w) for 20k PEO, theory predicts [12], and we observe, that the polymer can be forced inside the MTs. This occurs because, at such high polymer concentrations, the PEO in solution interacts with and crowds itself, so the relative cost of further confinement inside the MT lumen decreases [12]. Thus 20k PEO can enter the MT lumen at high concentrations, so there is no longer a pressure difference between the inside and outside of the MTs, and the MTs revert to a circular cross section.

This interpretation is supported by a number of additional experiments. We directly show that 20k PEO does

not associate with or enter the rectangular phase by mixing MTs with fluorescently labeled 20k PEO, where the bundles appear dark in fluorescence Fig. 1(e) [Fig. 1(d), corresponding DIC image]. When the bundles are in the hexagonal phase, the background appears uniformly bright, as would be expected if the labeled PEO enters the MTs (data not shown). When 600 PEO, a polymer with a radius of gyration of ~1 nm [10], much smaller than the MT inner radius, is used instead of 20k PEO, the nematic phase is seen below 30% (w/w) 600 PEO and only the hexagonal phases are seen with higher concentrations of 600 PEO. When a larger polymer with a radius of gyration of ~18 nm [10], 100k PEO, is used, only the nematic and rectangular phase are observed. Also, if the 20k PEO is separated from the MTs by a semipermeable membrane, then only the nematic and rectangular phase are present, and the measured $P_{cr}$ is similar to the value obtained when 20k PEO is directly added to the MTs. The reentrant hexagonal phase of MTs is never observed with 100k PEO or when 20k PEO is separated from the MTs by a semipermeable membrane.

Figure 3 shows the phase diagram as a function of osmotic pressure exerted by 20k PEO, obtained by mixing polymerized MTs with PEO. Publicly available data were used to determine the osmotic pressure of a given concentration of 20k PEO [13]. In the rectangular phase, the microtubules become more distorted as the osmotic pressure increases: $a_R$ decreases, $a_R \propto -1.22$ nm $\log(P)$, and $b_R$ increases, $b_R \propto 3.62$ nm $\log(P)$ (best fits, Fig. 3). Assuming elliptical cross sections for the MTs, and that there is 2 nm of water between MTs, the calculated perimeter of the buckled MTs deviates by less than 20% from the perimeter of an undistorted MT. In the hexagonal phase, increasing the osmotic pressure causes the separation between MTs, $a_H$, to decrease. This can be used to calculate the force per unit length between MTs [5], which is well fit by an exponential (dashed line, Fig. 3), $F = 7.2 \times 10^{-2}$N/m $\exp(-D/1.44\ \text{nm})$. Here $D$ is the separation between MT walls and the MTs were taken to have an outer radius of $R = 12.7$ nm [11]. This result is in remarkable agreement with the force per unit length predicted [14,15] between two charged cylinders [16] of this radius by Poisson-Boltzmann theory, assuming constant surface potential: $F = 5.2 \times 10^{-2}$N/m $\exp(-D/1.47\ \text{nm})$.

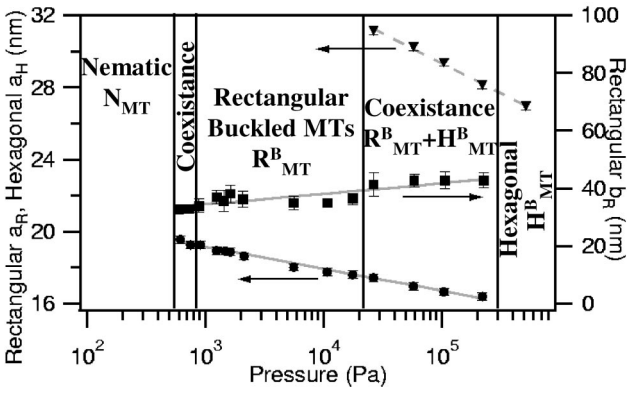


FIG. 3. Phase diagram of MTs with 20k PEO as a function of osmotic pressure. The lattice constants of the bundle phases change with pressure. For rectangular bundles, $a_R$ defines the smaller center-to-center distance (circles, left axis) and $b_R$ is the larger center-to-center distance (squares, right axis). $a_H$ is the center-to-center distance in the hexagonal phase (triangles, left axis).

$P_{cr}$ provides a measure of the mechanical properties of MTs. Previous experiments have measured the axial bending rigidity of MTs [17] (but see [18]). If MTs are modeled as homogeneous, isotropic, hollow cylinders with an outer radius $R = 12.7$ nm and a wall thickness of $h = 4.0$ nm [11], then the measured flexural rigidity predicts a Young's modulus of $E \sim 1.6$ GPa [17]. Assuming a Poisson ratio of $\upsilon = 0.4$ (similar to nylon), this model predicts $P_{cr} = Eh^3/4(1-\upsilon^2)R^3 = 14.8$ MPa [19], which is over 4 orders of magnitude greater than our measured $P_{cr}$. This apparent discrepancy is due to the fact that MTs are not homogeneous or isotropic. Specifically, the bonds between protofilaments are expected to be much weaker than the bonds within the tubulin dimer. The measured Young's modulus, along with cryoelectron microscopy measurements [11], indicates that resistance

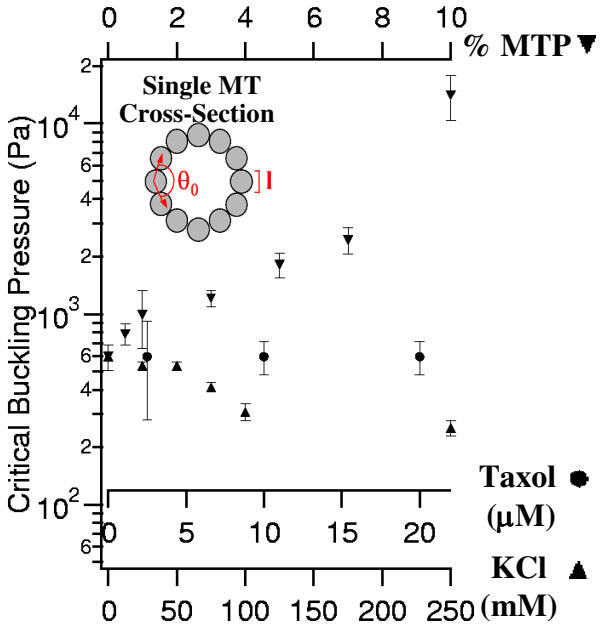


FIG. 4 (color online). The effect of solution conditions on the critical buckling pressure of MTs, $P_{cr}$. Added KCl (upward triangles) decreases $P_{cr}$. Polymerizing highly purified tubulin with MT protein (MTP = 20% MAP/80%tubulin w/w) leads to a large increase in $P_{cr}$ (downwards triangles, percent MTP by weight). $P_{cr}$ is unaffected by changes in the concentration of the chemotherapy drug taxol (circles). Cartoons display a single MT cross section.

to axial bending is dominated by deformation of the tubulin subunit [17]. This strongly suggests that the resistance to buckling due to radial osmotic pressure is caused by the lateral interactions between protofilaments in the MT lattice.

An estimate of the bending modulus of the bond between protofilaments may be obtained using a simple model. We model the MT cross section as composed of incompressible tubulin subunits of diameter $l \sim 5.0$ nm, connected by springs of spring constant $k$, which enforce a desired angle, $\theta_0$, between the subunits (see Fig. 4). For simplicity, we assume 12 protofilaments, which allows fourfold symmetry to be enforced. A linear elastic stability analysis results in a $P_{\mathrm{cr}} \sim 0.81k/l^2$ [19]. For our measured $P_{\mathrm{cr}}$ this leads to a very small $k \sim 4.4 \times 10^{-3} k_B\, T/\mathrm{nm}$ implying that ~28 tubulin dimers must stack to resist thermal fluctuations. Further work should include more sophisticated modeling such as imperfections in the MT lattice like the seam, interactions between MTs, finite temperature effects, and the distribution in protofilament number.

The value of $P_{\mathrm{cr}}$ is strongly affected by solution conditions. Adding monovalent salt decreases $P_{\mathrm{cr}}$ (Fig. 4, upwards triangles). This is expected since many of the lateral interactions between protofilaments are electrostatic [11]. When MTs are polymerized from mixtures of tubulin and microtubule protein (MTP), which is ~30% MAPs, 70% tubulin by weight, even small amounts of MTP greatly increase $P_{\mathrm{cr}}$. A mixture of 90% tubulin with 10% MTP is only ~3% MAPs by weight, yet the osmotic pressure required to buckle such MTs is over 20 times greater than the pressure required to buckle MTs polymerized from pure tubulin (Fig. 4, downwards triangles). This large effect of MAPs on the radial mechanical properties of MTs contrasts with their minor effect on the axial mechanical properties of MTs: Axial bending experiments show that MTs *fully saturated* with MAPs show an increase in flexural rigidity of only ~50% [17]. This implies that MAPs stabilize MTs by increasing the lateral interaction between protofilaments, perhaps by directly cross-linking them.

Using different concentrations of taxol to stabilize MTs after assembly does not affect $P_{\mathrm{cr}}$ (Fig. 4, circles). This indicates that taxol does not influence the strength of interprotofilament bonds at the concentrations used, even though MT polymerization is greatly effected [3]. Thus taxol stabilizes MTs by a different mechanism from MAPs, which we have demonstrated greatly increase the interaction between protofilaments. Our results are consistent with a model in which taxol functions by preventing the straight-to-curved conformational change in tubulin normally associated with GTP hydrolysis [4].

Understanding the roles played by distinct MAPs and drugs in controlling the organization and polymerization of MTs is of crucial biological and medical importance. By using the SAXRD-osmotic stress technique to determine the value of $P_{\mathrm{cr}}$ of MTs exposed to various agents, we have developed a method to measure interprotofilament interactions. This, in combination with mechanical measurements of the MT wall and the interactions between MTs, which are also obtained with this technique, introduces a new methodology for determining the mechanism of action of MT binding drugs and MAPs. A more detailed paper describing this work is in preparation [20].

We acknowledge insightful discussions with Bob McMeeking and Robijn Bruinsma. Supported by NIH GM-59288 and NS-13560, NSF DMR-0203755, CTS-0103516, and CTS-0404444. DOE supports SSRL. NSF-DMR-0080034 supports the UCSB MRL.

*Electronic address: safinya@mrl.ucsb.edu

[1] A. Desai and T. Mitchison, Annu. Rev. Cell Dev. Biol. **13**, 83 (1997).
[2] V. M. Y. Lee *et al.*, Annual Review of Neuroscience **24**, 1121 (2001).
[3] B. W. Derry *et al.*, Biochemistry **34**, 2203 (1995).
[4] L. A. Amos and J. Lowe, Chemistry & Biology **6**, R65 (1999).
[5] V. A. Parsegian *et al.*, Methods Enzymol. **259**, 43 (1995).
[6] S. Asakura and F. Oosawa, J. Polym. Sci. **33**, 183 (1958).
[7] J. C. Lee, L. L. Y Lee, Biochemistry **18**, 5518 (1979).
[8] J. M. Andreu *et al.*, J. Mol. Biol. **226**, 169 (1992); A. Marx *et al.*, Cell Mol. Biol. (Oxford) **46**, 949 (2000).
[9] S. Leibler *et al.*, Phys. Rev. Lett. **59**, 1989 (1987); S. G. Zhang, J. Phys. Soc. Jpn. **68** , 3603 (1999); U. Seifert, Phys. Rev. A **43**, 6803 (1991).
[10] K. Devanand and J. Selser, Macromolecules **24**, 5943 (1991).
[11] H. Li *et al.*, Structure **10**, 1317 (2002); D. Chretien *et al.*, Eur. Biophys. J. **27**, 490 (1998).
[12] E. F. Casassa, J. Polym. Sci. B **5**, 773 (1967); M. Daoud and P. G. De Gennes, J. Phys. (France) **38**, 85 (1977).
[13] R. Peter Rand, Osmotic Stress http://www.brocku.ca/researchers/peter_rand/osmotic/osfile.html#data.
[14] The surface charge of MTs at $p$H 6.8 is estimated as $-0.87\ e/\mathrm{nm}^2$, calculated from $\alpha\beta$-tubulin's primary structure in the PDB, including bound nucleotides. The salts are 40 mM Na PIPES and 0.5 mM $MgCl_2$ (as in our buffer).
[15] D. Leckband and J. Israelachvili, Q. Rev. Biophys. **34**, 105 (2001).
[16] R. Stracke *et al.*, Biochem. Biophys. Res. Commun. **293**, 602 (2002).
[17] B. Mickey and J. Howard, J. Cell Biol. **130**, 909 (1995).
[18] P. J. de Pablo *et al.*, Phys. Rev. Lett. **91**, 098101 (2003).
[19] E. Ventsel and T. Krauthammer, *Thin Plates and Shells* (Marcel Dekker, New York, 2001); L. Landau and E. Lifshitz, *Theory of Elasticity* (Pergamon, New York, 1975).
[20] D. J. Needleman *et al.* (to be published).